

Fast Reference-Based MRI

Lior Weizman, *Member, IEEE*, Yonina C. Eldar, *Fellow, IEEE*, and Dafna Ben Bashat

Abstract—In many clinical MRI scenarios, existing imaging information can be used to significantly shorten acquisition time or to improve Signal to Noise Ratio (SNR). In some cases, a previously acquired image can serve as a reference image, that may exhibit similarity to the image being acquired. Examples include similarity between adjacent slices in high resolution MRI, similarity between various contrasts in the same scan and similarity between different scans of the same patient. In this paper we present a general framework for utilizing reference images for fast MRI. We take into account that the reference image may exhibit low similarity with the acquired image and develop an iterative weighted approach for reconstruction, which tunes the weights according to the degree of similarity. Experiments demonstrate the performance of the method in three different clinical MRI scenarios: SNR improvement in high resolution brain MRI, utilizing similarity between T2-weighted and fluid-attenuated inversion recovery (FLAIR) for fast FLAIR scanning and utilizing similarity between baseline and follow-up scans for fast follow-up scanning.

Index Terms—Compressive sensing and sampling, Magnetic resonance imaging (MRI), Brain.

I. INTRODUCTION

Magnetic resonance imaging (MRI) data is sampled in the spatial Fourier transform (a.k.a. k-space) of the object under investigation. In many cases, the k-space is sampled below Nyquist rate due to constraints in the implementation of the k-space trajectory that controls the sampling pattern (e.g., acquisition duration and smoothness of gradients). Mostly, prior assumptions on the nature of the data are taken into account in the reconstruction process, to overcome imaging artifacts due to insufficient sampling.

Since the introduction of Compressed Sensing (CS) [1], [2], [3], [4] to the field of MRI [5], many MRI reconstruction approaches exploit the fact that MR images are highly compressible, by formalizing the image reconstruction problem as an ℓ_1 minimization problem. We can roughly divide these MRI reconstruction approaches into two families: single- and multiple-image sparsity-based recovery.

The first family of methods exploits the sparsity of a single MR image in some transform domain. Wavelet transform has been widely used as a sparsifying transform for brain MRI. Total Variation (TV) has been used for MR images which are sparse in the image domain, such as angio-MRI [5], [6]. Other approaches focus on learning the sparsifying transform or using a dictionary developed exclusively for MRI. While these approaches were among the first ones to utilize CS

L. Weizman and Y.C. Eldar are with the Department of Electrical Engineering, Technion - Israel Institute of Technology, Israel; e-mail: weizman@tx.technion.ac.il.

D. Ben Bashat is with the MRI research center of Tel-Aviv University.

This work was supported by the Ministry of Science and by the ISF I-CORE joint research center of the Technion and the Weizmann Institute, Israel.

for MRI, they still suffer from artifacts in cases of severe undersampling.

The second family of methods exploits similarity within a series of MRI images. In dynamic imaging, MRI images are acquired at high frame rate. This allows the exploitation of the sparsity of Fourier transform along the temporal dimension, assuming that only parts of the field-of-view (FOV) change at a high temporal rate [7]. Dynamic MRI can also be inherently represented as a superposition of a low-rank, static background component and a sparse dynamic component [8]. This leads to improved results in CS for dynamic MRI, as sparsity is enforced only on the sparse components of the image [9]. In multiple-contrast MRI, structural similarity between different contrasts in the same scan is assumed. This similarity is exploited by enforcing sparsity on the gradient images of different imaging contrast [10], [11].

Multiple-image sparsity-based reconstruction is application dependent; since similarity between multiple images takes different forms, a unique sparsity-based reconstruction was developed for each MRI application, exploiting its specific sparse nature. No general sampling and reconstruction scheme which fits a variety of multiple-image MRI applications has been developed so far. Moreover, most of the methods rely on the assumption that there is substantial similarity between the images in the series, in the image or in some transform domain. This assumption may not be valid in some cases and can lead to undesired reconstruction results. In addition, the parameters of ℓ_1 -based MRI reconstruction problems are determined in advance, and are not optimized during the reconstruction process. Optimization of parameters during reconstruction may highly increase the matching of the ℓ_1 model to the measurements, as will be demonstrated later in this paper.

While CS-based MRI reconstruction approaches mainly focus on time saving by k-space undersampling, reducing the number of repetitions in MRI can be a substantial source for time saving. Many high resolution MRI applications suffer from low Signal to Noise Ratio (SNR) and require averaging over multiple scanning repetitions for adequate SNR. These repetitions may double or triple the total scanning time. SNR improvement has been addressed in the MRI literature mainly by improving the hardware or the acquisition process itself. In this paper we show that our framework is applicable for reducing the number of repetitions in low-SNR MRI applications, and significantly shortens the total scanning time.

Recently, we introduced an iterative approach for sampling and reconstruction exploiting similarity across multiple MRIs of the same patient [12]. We considered the acquisition of a follow-up MRI, given the baseline scan of the same patient. We took into account that baseline and follow-up images may not exhibit similarity and developed an iterative weighted

mechanism that adjusts the reconstruction parameters and the sampling locations during real-time scanning. While the idea of optimizing the sampling locations has also been proposed by others [13], it suffers from practical difficulties due to the necessity to solve many computationally heavy ℓ_1 minimization problems during the acquisition process.

In related work [14], we have shown that enforcing similarity between adjacent, low SNR, thin MRI slices, can lead to significant improvement in SNR that obviates the need for multiple repetitions for high SNR. Our approach is based on modifying the RF pulse signal for different weighting of the thin slices in the acquired data, which might be difficult in practical implementation in existing MRI hardware. In this paper we extend the ideas presented in our previous publications for the development of a general scheme that utilizes similarity to a reference image for a variety of MR imaging applications.

More specifically, we introduce a general framework, called "fast reference-based MRI" which is based on two main elements: (a) exploiting both sparsity in the wavelet domain and similarity to a reference scan and; (b) weighted reconstruction by adaptive selection of weights during the reconstruction process, taking into account the degree of similarity to the reference image.

This framework is used to shorten the acquisition time for many MRI applications in which a reference image, known in advance, is available. The reference image may exhibit some degree of similarity with the data we intend to acquire. Unlike existing methods that are application-specific and require high degree of similarity to the prior, our approach requires no assumptions regarding the similarity of the reference image with the acquired data. The adaptive weights in our framework adapt the reconstruction to the actual similarity between the scans. Therefore, it fits a variety of clinical imaging applications with supplemental imaging information, that in many cases is neglected due to its low fidelity.

Experimental results demonstrate the applicability of the proposed method in three different scenarios that utilize similarity to a reference image. The first application exploits similarity between two different imaging contrasts for fast scanning of one of them. The second application exploits similarity between different scans of the same patient for fast scanning of follow-up scans, and the third application exploits similarity between adjacent slices to improve SNR within the same imaging contrast.

A major contribution of the SNR improvement applications is that it speeds-up the acquisition without the need to undersample the k-space. It is based on images acquired with less repetitions than conventional ones. Therefore, it requires no pulse sequence programming and can be applied for standard pulse sequences used today in the clinic. Unlike undersampling-based approaches, this implementation has the potential for smooth and fast penetration into the clinical environment.

This paper is organized as follows. Section II presents the proposed reference-based MRI approach. Section IV describes the experimental results. Section V discusses the method and its results and Section VI concludes by highlighting the key

findings of the research.

II. REFERENCE-BASED MRI

A. Compressed Sensing MRI

The application of CS for MRI [5] exploits the fact that MRI scans are typically sparse in some transform domain, which is incoherent with the sampling domain. Nonlinear reconstruction is then used to enforce both sparsity of the image representation in some transform domain and consistency with the acquired data. A typical formulation of CS MRI recovery aims to solve the following constrained optimization problem:

$$\min_{\mathbf{x}} \|\Psi \mathbf{x}\|_1 \text{ s.t. } \|\mathbf{F}_u \mathbf{x} - \mathbf{y}\|_2 < \epsilon \quad (1)$$

where $\mathbf{x} \in \mathbb{C}^N$ is the N -pixel complex image to be reconstructed, represented as a vector, $\mathbf{y} \in \mathbb{C}^M$ represents the k-space measurements, \mathbf{F}_u is the undersampled Fourier transform operator, Ψ is a sparsifying transform operator and ϵ controls the fidelity of the reconstruction to the measured data. We further consider brain MRI, known to be sparse in the wavelet domain. Therefore, we will assume throughout that Ψ is an appropriately chosen wavelet transform.

In many cases, CS-MRI is solved in its so-called Lagrangian form, where λ is a properly chosen regularization parameter:

$$\min_{\mathbf{x}} \|\mathbf{F}_u \mathbf{x} - \mathbf{y}\|_2^2 + \lambda \|\Psi \mathbf{x}\|_1. \quad (2)$$

This fundamental CS MRI formulation is the basis for many MRI reconstruction applications, where the sparse transform domain varies depending on the particular setting [15], [16], [7], [17]. We note that this basic formulation does not take into account any image-based prior information, that exists in many MRI applications.

B. Reference-based compressed sensing MRI

In many MRI imaging scenarios, an a-priori image that may exhibit similarity to the acquired image, is available. This image is coined hereinafter the "reference image" and represented as \mathbf{x}_0 . A reference image could be a different imaging contrast in the same scan, an adjacent image slice or a previous scan of the same patient.

In some imaging applications, we can assume that \mathbf{x}_0 and \mathbf{x} are similar in most image regions [7]. Therefore the difference: $\mathbf{x} - \mathbf{x}_0$ can be modeled as sparse, and a CS based optimization utilize the reference image for improved reconstruction, via ℓ_1 minimization. Such a reference-based compressed sensing takes into account the fidelity of the measurements and the similarity to the reference scan, as follows:

$$\min_{\mathbf{x}} \|\mathbf{F}_u \mathbf{x} - \mathbf{y}\|_2^2 + \lambda \|\mathbf{x} - \mathbf{x}_0\|_1. \quad (3)$$

This optimization problem assumes high degree of similarity between \mathbf{x}_0 and \mathbf{x} , and is therefore suitable for some specific MRI applications, such as dynamic MRI. However, many MRI applications do not utilize available reference imaging information (for instance, by using (3)) due to the fact that the similarity to the acquired image is partial, not guaranteed or unknown. Examples include similarity between different

imaging contrasts in the same scan and consecutive scans of patients under clinical follow-up.

We introduce a general framework for reference based MRI, which takes into account the fact that \mathbf{x}_0 may exhibit differences versus \mathbf{x} . We also take into account that not all the samples in \mathbf{y} have the same SNR; we want to prioritize samples with high SNR over low SNR ones in the reconstruction process. Our approach is based on enforcing similarity between \mathbf{x} and \mathbf{x}_0 via weighted ℓ_1 norm, as follows:

$$\min_{\mathbf{x}} \|\mathbf{A}(\mathbf{F}_u \mathbf{x} - \mathbf{y})\|_2^2 + \lambda_1 \|\mathbf{W}_1 \Psi \mathbf{x}\|_1 + \lambda_2 \|\mathbf{W}_2(\mathbf{x} - \mathbf{x}_0)\|_1 \quad (4)$$

where \mathbf{A} is a diagonal matrix that controls the weight given to the fidelity of certain measurements (used to prioritize samples with high SNR). The matrices \mathbf{W}_1 and \mathbf{W}_2 are weighting matrices, $\mathbf{W}_k = \text{diag}([w_k^1, w_k^2, \dots, w_k^N])$ with $0 \leq w_k^i \leq 1$, that control the weight given to each element in the sparse representation.

In particular, \mathbf{W}_1 is used to weight specific wavelet atoms in the reconstruction process and \mathbf{W}_2 is used to weight image regions according to their similarity level with the reference scan. The parameters λ_1 and λ_2 are regularization parameters that control the weight given to each term in the optimization problem.

In most cases, the expected SNR of the acquired data is known and the matrix \mathbf{A} can be determined in advance. As to \mathbf{W}_1 and \mathbf{W}_2 , there are cases in which neither the similarity to the reference image nor the support in the wavelet domain are known in advance, and therefore these weighting matrices have to be determined during the acquisition process as we describe in the next section.

C. Adaptive weighting for reference based MRI

Since the similarity of \mathbf{x} to \mathbf{x}_0 , as well as the support of \mathbf{x} in wavelet domain, are unknown, we estimate the matrices \mathbf{W}_1 and \mathbf{W}_2 from the acquired data, in an adaptive fashion. Inspired by Weighted-CS [18], we propose an iterative algorithm, where in each iteration a few k-space samples are added to the reconstruction process, and priority is given to samples closer to the origin of the k-space. Then, $\hat{\mathbf{x}}$ is estimated, to serve as the basis for estimating the weighting matrices in the next iteration.

Our rational behind the iterative computation of \mathbf{W}_k is as follows. For \mathbf{W}_1 , we would like to relax the demand for sparsity on elements in the support of $\Psi \mathbf{x}$. For \mathbf{W}_2 , we would like to enforce sparsity only in spatial regions where $\mathbf{x} \approx \mathbf{x}_0$. Since \mathbf{x} is unknown, $\hat{\mathbf{x}}$, updated in every iteration, is used instead. Therefore, the elements of the weighting matrices are chosen as follows:

$$\begin{aligned} w_1^i &= \frac{1}{1 + [|\Psi \hat{\mathbf{x}}|]_i} \\ w_2^i &= \frac{1}{1 + [|\hat{\mathbf{x}} - \mathbf{x}_0|]_i} \end{aligned} \quad (5)$$

where $[\cdot]_i$ denotes the i th element of the vector in brackets. We note that in a similar way to Candès' approach [18], developed for \mathbf{x} which is truly sparse, the weights in (5) are given values that vary between 0 and 1. The values for w_1^i and w_2^i

are inversely proportional to the values of the corresponding elements in the vectors $\Psi \mathbf{x}$ and $\hat{\mathbf{x}} - \mathbf{x}_0$, respectively.

The proposed algorithm is coined Fast Reference-Based MRI and is summarized in Algorithm 1. Note that in the first iteration of the algorithm we do not assume similarity with the reference image (i.e., we set $\mathbf{W}_1 = \mathbf{I}$ and $\mathbf{W}_2 = \mathbf{0}$ for the first iteration).

Algorithm 1 Fast Reference-Based MRI

Input:

Number of iterations: N_I ; Reference image: \mathbf{x}_0

Sampled k-space: \mathbf{z} ; Tuning constants: λ_1, λ_2

Number of k-space samples added at each iteration: N_k

Expected fidelity of measurements: \mathbf{A}

Output:

Estimated image: $\hat{\mathbf{x}}$

Initialize:

$\mathbf{W}_1 = \mathbf{I}$, $\mathbf{W}_2 = \mathbf{0}$;

Reconstruction:

for $l = 1$ to N_I do

 Add N_k new samples to \mathbf{y} from \mathbf{z} according to distance from center of k-space.

Weighted reconstruction: Estimate $\hat{\mathbf{x}}$ by solving (4)

Update weights: Update \mathbf{W}_1 and \mathbf{W}_2 according to (5)

end for

To solve the ℓ_1 -minimization problem (4) in the weighted reconstruction phase, we use an extension of SFISTA [19]. The extended algorithm is summarized in Algorithm 2, where the notation $\|\cdot\|_2$ for matrices denotes the largest singular value. The operator $\Gamma_{\lambda\mu}(\mathbf{z})$ is the soft shrinkage operator, which operates element-wise on \mathbf{z} and defined as (for complex valued z_i):

$$\Gamma_{\lambda\mu}(z_i) = \begin{cases} \frac{|z_i| - \lambda\mu}{|z_i|} z_i, & |z_i| > \lambda\mu \\ 0, & \text{otherwise.} \end{cases} \quad (6)$$

Algorithm 2 minimizes (4), where the trade-off between the two sparsity assumptions is controlled by the ratio between λ_1 and λ_2 , via $\Gamma(\cdot)$, and the overall convergence is controlled by μ .

III. REFERENCE-BASED MRI FOR SNR IMPROVEMENT

In MRI, SNR is proportional to the number of protons involved in generating the measured signal. As a result, thick slices provide better SNR than thin ones. However, the thinner the slice, the better the image resolution in the z-axis. Therefore, to obtain high quality MRI for clinical evaluation purposes, high SNR MRI that consists of thin slices is required. The common approach today for SNR improvement of MRI with thin slices consists of averaging over several repetitions, (usually three or four repetitions) which extends the scanning time in the same ratio.

In this application, where thin slices are acquired, one may consider shortening scanning time by reducing the number of repetitions and exploiting similarity between thin slices. In addition, similarity to thick, high SNR image slice that overlaps the thin slices can also be utilized for SNR improvement.

Algorithm 2 SFISTA algorithm for Reference-based MRI**Input:**k-space measurements: \mathbf{y} Sparsifying transform operator: Ψ An $N \times N$ k-space undersampling operator: \mathbf{F}_u Reference image: \mathbf{x}_0 Expected fidelity of measurements: \mathbf{A} Tuning constants: $\lambda_1, \lambda_2, \mu$ An upper bound: $L \geq \|\mathbf{A}\mathbf{F}_u\|_2^2 + \frac{\|\mathbf{W}_1\Psi\|_2^2 + \|\mathbf{W}_2\|_2^2}{\mu}$ **Output:** Estimated image: $\hat{\mathbf{x}}$ **Initialize:**

$$\mathbf{x}_1 = \mathbf{z}_2 = \mathbf{F}_u^*\mathbf{y}, t_2 = 1$$

Iterations:**Step k:** ($k \geq 2$) Compute

$$\nabla f(\mathbf{z}_k) = \mathbf{A}^*(\mathbf{F}_u^*(\mathbf{A}(\mathbf{F}_u\mathbf{z}_k - \mathbf{y})))$$

$$\nabla g_{1\mu}(\mathbf{W}_1\Psi\mathbf{x}_{k-1}) = \frac{1}{\mu}\mathbf{W}_1\Psi^*(\mathbf{W}_1\Psi\mathbf{x}_{k-1}) - \Gamma_{\lambda_1\mu}(\mathbf{W}_1\Psi\mathbf{x}_{k-1})$$

$$\nabla g_{2\mu}(\mathbf{W}_2(\mathbf{x}_{k-1} - \mathbf{x}_0)) = \frac{1}{\mu}\mathbf{W}_2(\mathbf{W}_2(\mathbf{x}_{k-1} - \mathbf{x}_0) - \Gamma_{\lambda_2\mu}(\mathbf{W}_2(\mathbf{x}_{k-1} - \mathbf{x}_0)))$$

$$\mathbf{x}_k = \mathbf{z}_k - \frac{1}{L}(\nabla f(\mathbf{z}_k) + \nabla g_{1\mu}(\mathbf{W}_1\Psi\mathbf{x}_{k-1}) + \nabla g_{2\mu}(\mathbf{W}_2(\mathbf{x}_{k-1} - \mathbf{x}_0)))$$

$$t_{k+1} = \frac{1 + \sqrt{1 + 4t_k^2}}{2}$$

We will consider a specific implementation, where a single repetition is used to acquire two thin adjacent slices with low SNR, \mathbf{x}_1 and \mathbf{x}_2 , and a single thick slice, \mathbf{x}_3 that spatially overlaps \mathbf{x}_1 and \mathbf{x}_2 . Obviously, our goal is to improve the SNR of \mathbf{x}_1 and \mathbf{x}_2 taking into account the similarity between them and the high-SNR, thick slice, \mathbf{x}_3 . In this specific example we perform a total of three acquisitions for high SNR reconstruction of two adjacent slices, instead of 8 acquisitions (4 repetitions for each thin slice) in the conventional, repetition-based approach.

To introduce our approach within our framework, let

$$\mathbf{y} = \begin{bmatrix} \mathbf{y}_1 \\ \mathbf{y}_2 \\ \mathbf{y}_3 \end{bmatrix}, \quad \mathbf{x} = \begin{bmatrix} \mathbf{x}_1 \\ \mathbf{x}_2 \\ 0.5(\mathbf{x}_1 + \mathbf{x}_2) \end{bmatrix} \quad (7)$$

where \mathbf{y} represents the k-spaces of two thin slices and the corresponding thick one, respectively, and \mathbf{x} represents the two thin slices and their average, which corresponds to the overlapping thin slice. The matrix \mathbf{A} is determined by the estimated SNR of the elements in \mathbf{y} , giving higher values for elements corresponding to \mathbf{y}_3 versus elements that correspond to \mathbf{y}_1 and \mathbf{y}_2 . Similarity is enforced between the thin slices, and (4) is reformulated as:

$$\min_{\mathbf{x}} \|\mathbf{A}(\mathbf{F}_3\mathbf{x} - \mathbf{y})\|_2^2 + \lambda_1 \|\mathbf{W}_1\Psi_3\mathbf{x}\|_1 + \lambda_2 \|\mathbf{W}_2\mathbf{B}\mathbf{x}\|_1. \quad (8)$$

Here $\mathbf{F}_3 = [\mathbf{F}, \mathbf{F}, \mathbf{F}]$, $\Psi_3 = [\Psi, \Psi, \Psi]$ and $\mathbf{B} = \text{diag}([1, \dots, \underbrace{1}_{N \text{ times}}, \underbrace{-1}_{N \text{ times}}, \dots, \underbrace{-10}_{N \text{ times}}, \dots, 0])$.

Note that similarity between the thick slice to the average between the thin slices is enforced in the Fourier domain, via the leftmost term of (8). Adapting Algorithm 1 and Algorithm 2 to solve (8) in iterative manner is straightforward and appears in the Appendix.

This formulation does not require k-space undersampling and therefore can be easily applied in most MR scanners using conventional pulse sequences. As opposed to random k-space undersampling that requires pulse sequence programming, our reference-based SNR improvement approach requires controlling the number of repetitions and slice thicknesses only, which is possible in most commercial MR scanners.

IV. EXPERIMENTAL RESULTS

To demonstrate the performance of our reference based MRI approach we examine three MRI applications, all of which utilize a reference scan for improved reconstruction. Where relevant, partial k-space acquisition was obtained by down-sampling a fully sampled k-space. We use a standard variable random sampling (VDS) scheme for simplicity and fast scanning. Random samples were taken according to probability density function (pdf) of the data, when we undersampled less in the center of the k-space according to polynomial density of order 4 [5]. A Daubechies-4 wavelet transform was used as the sparsifying transform. Different values of λ_1, λ_2 in the range of [0.001, 0.9] were examined, and the best result in terms of image quality is presented in each case. We used $\mu = 10^{-3}(\frac{\lambda_1 + \lambda_2}{2})^{-1}$ in our experiments. The number of iterations used in Algorithm 2 for the results obtained in this section is between 30 and 50 iterations.

All scans were performed on a GE Signa 1.5T HDx scanner. High SNR images reconstructed from fully sampled, multiple repetition data serve as gold standard. The source code and data required to reproduce the results presented in this paper can be downloaded from:

<http://www.technion.ac.il/~weizmanl/software>

A. Utilizing similarity between T2-weighted and FLAIR

In this experiment, our goal is to reconstruct a FLAIR image, \mathbf{x} , from undersampled measurements, utilizing similarity to a T2-weighted image. Images were acquired with an in-plane resolution of $0.5 \times 0.5 \text{ mm}^2$ and with slice thickness of 4 mm . We sampled only 15% of the FLAIR k-space with variable density random sampling and utilized a fully sampled T2-weighted scan as the reference image \mathbf{x}_0 . Since all samples were acquired with similar SNR, $\mathbf{A} = \mathbf{I}$.

FLAIR and T2-weighted scans are known to exhibit high similarity in regions with low fluid concentration. Therefore, while \mathbf{W}_2 can be computed iteratively as described in Algorithm 1, it is possible to save time in the reconstruction process by utilizing this information. To this end we give low values to elements in \mathbf{W}_2 corresponding to pixels with high fluid concentration and 1 to others. The regions with high fluid concentration can be easily detected by their high intensity values in the reference, T2-weighted image.

Figure 1 shows the fully sampled T2 and FLAIR images, reconstruction based on sparsity in the wavelet domain only (by solving (1) using undersampled FLAIR data only) and our reference based reconstruction using binary values for \mathbf{W}_2 (representing fluid/non fluid regions). It can clearly be seen that reference-based FLAIR reconstruction outperforms traditional wavelet sparsity based FLAIR recovery, using only 15% of the data.

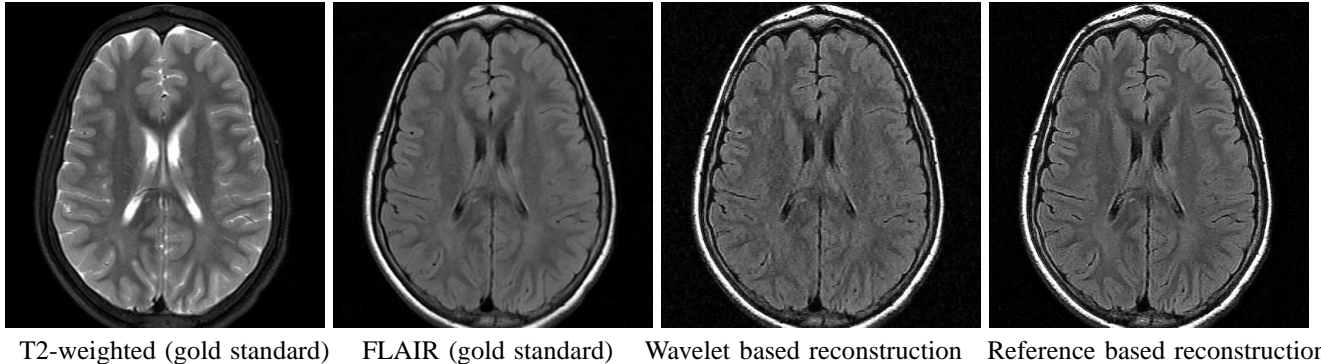


Fig. 1. Reference based MRI used within the same scan: reconstruction results utilizing similarity between T2 and FLAIR contrasts. The similarity between T2 and FLAIR in regions with low fluid concentration (demonstrated in the two leftmost images) is exploited for high quality reconstruction from 15% of k-space FLAIR data (rightmost image). State-of-the-art wavelet based reconstruction using the same data results in imaging artifacts (second from the right image).

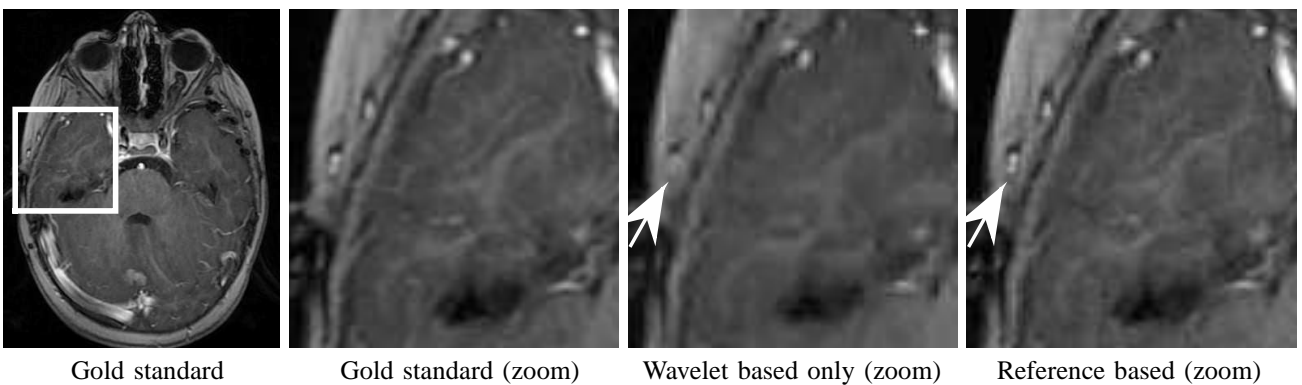


Fig. 2. Reference based MRI used in longitudinal studies: reconstruction results from 6% of k-space data. The enlarged region shown in the three rightmost images corresponds to the marked region in the leftmost image. It can be seen that our reference-based approach exhibits results which are very similar to the gold standard, and reveals imaging features that are not visible in state-of-the-art wavelet based MRI reconstruction.

B. Utilizing similarity between baseline of follow-up scans

Repeated brain MRI scans of the same patient every few weeks or months are very common for follow-up of brain tumors. Here, our goal is use a previous scan in the time series as a reference scan for reconstruction of a follow-up scan. In this application we need to tackle some practical problems such as grey-level variations and miss-registration between scans acquired at different dates. While these obstacles were discussed thoroughly in our previous publication [12] and in Section V-C of this paper, similarity between the reference and current scans is still not guaranteed (e.g. due to pathology changes), and prior information on spatial regions that may exhibit differences is not available.

Therefore, in this case we used all the features described in Section II-C and estimated \mathbf{W}_1 and \mathbf{W}_2 in an iterative manner. Since all samples were acquired with similar SNR, we set $\mathbf{A} = \mathbf{I}$.

Figure 2 shows reconstruction results of a follow-up T1-weighted brain scan utilizing the baseline scan as a reference scan (resolution: $0.5 \times 0.5 \text{ mm}^2$, thickness: 1 mm for both scans). Results were obtained using only 6% of k-space data. It can be seen that the reference based method exhibits imaging features that are hardly visible in the wavelet based reconstruction method. The superiority of our approach is achieved thanks to the iterative mechanism that adapts the

reconstruction to match actual similarity. This application has been thoroughly studied and analysed in our previous publication [12].

C. Utilizing similarity between adjacent slices

In this application we examine the extension of fast reference based MRI detailed in Section III to improve SNR of thin MRI slices. We acquired a brain T2-weighted scan with slice thickness of 0.8 mm followed by an additional acquisition with slice thickness of 1.6 mm . In all scans a single repetition was used and the in plane resolution was $0.8 \times 0.8 \text{ mm}^2$. As a result, we obtained a low SNR scan consisting of thin slices, and high SNR scan consisting of thick slices where each thick slice overlaps two thin ones. Our goal is to reconstruct a high SNR scan comprised of thin slices from this data.

Figure 3 shows thin slices at various SNR levels, and the corresponding reconstruction results. In terms of scanning time, 4 repetitions are required to obtain thin slices with SNR comparable to SNR of data reconstructed with our method. Therefore, without additional acceleration approaches (parallel imaging etc.), our approach requires scanning 3 slices once versus scanning 2 slices 4 times in conventional scanning, yielding a speed-up factor of 2.6 for the proposed method.

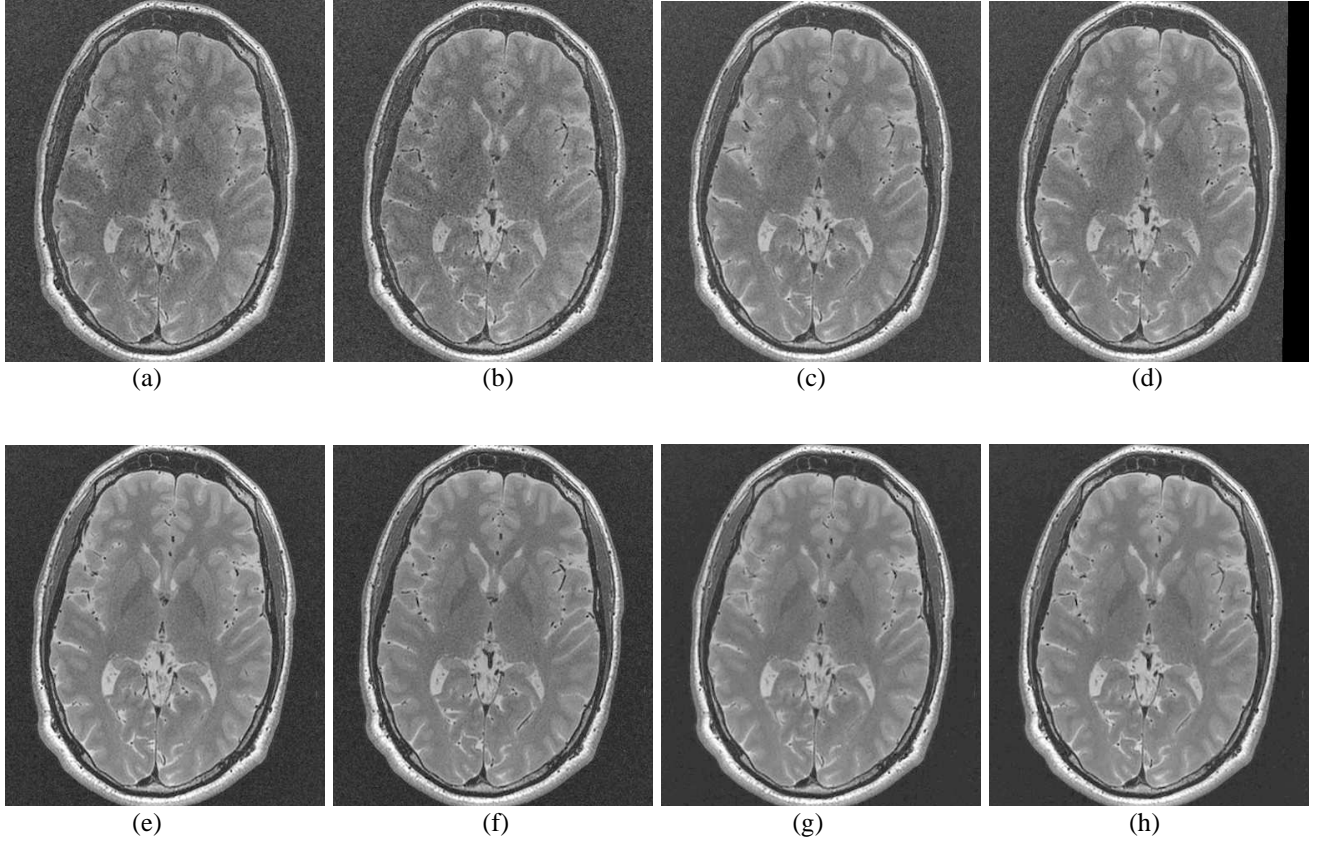


Fig. 3. Reference based MRI used within the same imaging contrast: reconstruction results from low SNR data. The pairs (a)-(b), (c)-(d) and (e)-(f) show two adjacent thin T2-weighted slices acquired with one, two and four repetitions, respectively. High similarity exists within pairs which can be exploited to improve SNR. It can be seen that at least four repetitions are required for adequate SNR. The pair (g)-(h) shows the results of our reference-based method, obtained by exploiting similarity between (a) and (b) and a high SNR thick slice (not shown). It can be seen that SNR is significantly improved and comparable to four repetitions images.

D. Parameter sensitivity analysis

In this analysis we examine the sensitivity of reference-based MRI to changes in the parameters, and provide quantitative measures for our experimental results. We examine the peak signal-to-noise ratio (PSNR) results of each experiment for various values of λ_1 and λ_2 . In this analysis, PSNR is defined as: $PSNR = 10\log_{10}(M^2/V_s)$, where M denotes the maximum possible pixel value in the image and V_s is the Mean Square Error (MSE) between the original image, \mathbf{x} and the reconstructed image, $\hat{\mathbf{x}}$.

Fig. 4 shows the PSNR results. The values shown for the adjacent slices experiment were averaged over the two thin slices used in the experiment. Generally, we can say that lower values of λ_1 and λ_2 (< 0.1) provide better PSNR than higher ones. This can be explained by the fact that over-promoting sparsity versus consistency to measurements degrades the reconstruction quality. In addition, we see that the T2-FLAIR experiment provides a lower range of PSNR values in comparison to other experiments. This can be explained by the fact that similarity is not enforced over the entire image in this case, due to many regions of differences between FLAIR and T2.

It can be seen that for $\lambda_1, \lambda_2 \in [0.001, 0.005]$ we obtain high PSNR, regardless of the specific application the method

is used for. This may indicate the optimal range of values for these parameters and obviate the need for optimization in future applications of reference-based MRI.

V. DISCUSSION

A. Adaptive sampling

While in our approach all data is acquired at once. Several recent publications suggest that prior knowledge can also be used to optimize the data acquisition [20], [21], [22]. However, since in our framework the similarity between scans is not guaranteed, we avoid using prior information during sampling. Another way of utilizing the reference image in the sampling stage would be to acquire a small number of samples in each iteration based on the reconstruction results, in an adaptive manner [23], [24], [25], [26], [13]. This approach, which requires image reconstruction at each iteration as part of the sampling process, has been tested in our previous work [12]. It was shown to be time consuming leading to substantial increase of scanning time if not programmed in hardware or accelerated by other means.

B. Possible extensions

This paper deals with the case of a single reference image used for reconstruction. However, we may utilize information from multiple reference images [27]. For example, it is

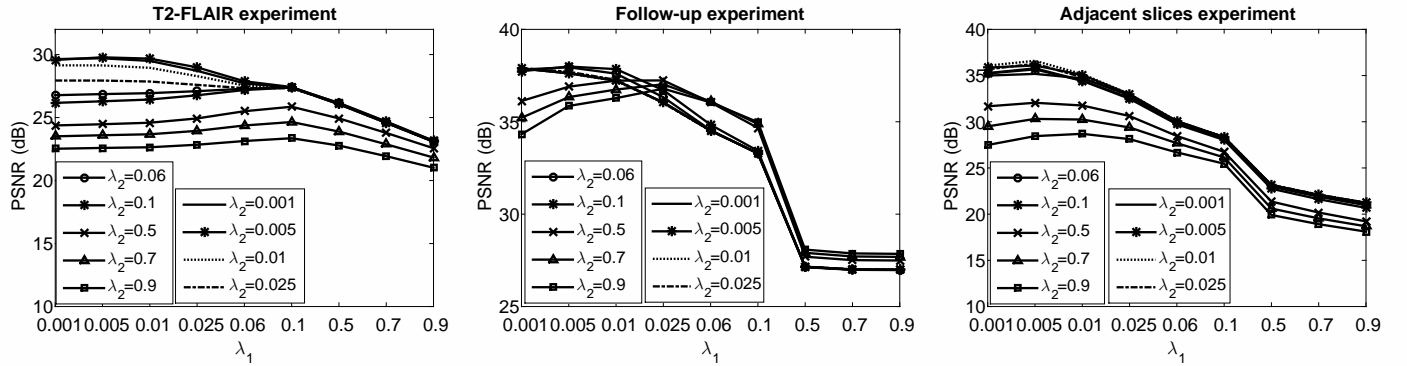


Fig. 4. Sensitivity analysis: PSNR results of T2-FLAIR (left), follow-up (middle) and adjacent slice (top) similarity applications for various values of λ_1 and λ_2 . It can be seen that $\lambda_1, \lambda_2 \in [0.001, 0.005]$ exhibits reliable results for all cases.

possible to extend the method to support similarity between multiple imaging contrasts in the same scan or to embed information from multiple scans to speed up longitudinal scanning. Extending our algorithm to support M reference images, $\mathbf{x}_{ref} = [\mathbf{x}_1^T, \dots, \mathbf{x}_M^T]^T$ can be performed by defining $\mathbf{x}_R = [\underbrace{\mathbf{x}^T, \dots, \mathbf{x}^T}_M]^T$ and modifying (4) as follows [28]:

$$\min_{\mathbf{x}} \|\mathbf{A}(\mathbf{F}_u \mathbf{x} - \mathbf{y})\|_2^2 + \lambda_1 \|\mathbf{W}_1 \Psi \mathbf{x}\|_1 + \lambda_2 \|\mathbf{W}_2 \mathbf{E}(\mathbf{x}_R - \mathbf{x}_{ref})\|_1 \quad (9)$$

where \mathbf{E} is a diagonal matrix,

$$\mathbf{E} = \text{diag}([\underbrace{e^{j \frac{2\pi}{M} 0}, \dots, e^{j \frac{2\pi}{M} 0}}_N, \dots, \underbrace{e^{j \frac{2\pi}{M} (M-1)}, \dots, e^{j \frac{2\pi}{M} (M-1)}}_N]) \quad (10)$$

which ensures that the each reference scan equally contributes to the minimization problem.

Another possible extension of this work can be to include prior knowledge based on user input regarding the level of similarity to the reference scan. For instance, in the follow-up application, the user may annotate the pathology region as an evolving region, that is likely to exhibit low level of similarity. As a result, the estimation of the weighting matrices will be more accurate, leading to improved performance of the method.

C. Practical limitations

Reference-based MRI assumes that the reference scan and acquired scan are spatially aligned and exhibit a similar range of grey-level intensities. While these assumptions are mostly valid within the same imaging contrast (our slice similarity application), they may not be valid for different contrasts or scans acquired at different times.

The solution to both issues can be obtained by grey-level normalization and realigning after acquisition. Since all data is acquired prior to reconstruction, a wavelet based recovery using all samples can be performed first. Although it may exhibit poor reconstruction of fine details (as presented in our experiments), it was found to be sufficient for grey-level normalization and alignment parameter extraction. Then, the

extracted parameters are used for normalization and realignment of the data in the reference-based MRI method for improved reconstruction performance.

It is worth noting here that if the alignment and normalization processes fail, our iterative approach will detect the low similarity between the scans. As a result, the reference image will not be taken into account and the result will converge to a wavelet-based reconstruction.

VI. CONCLUSIONS

In this paper we introduce a new framework for reference based MRI. We developed an iterative reconstruction approach that supports cases in which similarity to the reference scan is not guaranteed. We demonstrate the performance of our framework in three clinical MRI applications, including reconstruction from noisy images and from undersampled k-space data. Results exhibit significant improvement versus wavelet sparsity based MRI.

Many CS-MRI-based techniques consist of k-space undersampling and require sequence programming that may delay their penetration to the clinical environment. Moreover, in many cases sequence programmers have to compromise on sub-optimal undersampling patterns, since optimal methods may not be implementable in a real MRI scanner.

While two applications presented in this paper are also based on k-space undersampling, our SNR improvement application requires no undersampling in the k-space domain. It is based on images acquired with less repetitions than conventional ones. Therefore, it requires no pulse sequence programming and can be applied for standard pulse sequences used today in the clinic. Unlike undersampling-based methods, this implementation has the potential for smooth and fast penetration into the clinical environment.

Thanks to the existence of reference images in various clinical imaging scenarios, the proposed framework can play a major part in improving reconstruction in many MR applications. Future work will consist of applying the method to a wider range of medical imaging applications, such as low dose CT and fMRI.

APPENDIX A

ADAPTATION OF ALGORITHM 1 AND 2 FOR
REFERENCE-BASED SNR IMPROVEMENT.

The SNR improvement in Section III requires the solution of (8) in an iterative manner. For this purpose, we define the weights update as follows:

$$\begin{aligned} w_1^i &= \frac{1}{1 + [\|\Psi_3 \hat{x}\|]_i} \\ w_2^i &= \frac{1}{1 + [\|\mathbf{B} \hat{x}\|]_i}. \end{aligned} \quad (11)$$

Below we describe Algorithms 3 and 4, which are adaptations of Algorithms 1 and 2 to this setting, where $\Gamma_{\lambda\mu}(\mathbf{z})$ is defined in (6), $\mathbf{F}_3^* = [\mathbf{F}^*, \mathbf{F}^*, \mathbf{F}^*]$ and $\Psi_3^* = [\Psi^*, \Psi^*, \Psi^*]$.

Algorithm 3 Reference-based MRI for SNR improvement

Input:

Fully sampled k-space of \mathbf{x} : \mathbf{z} ; Tuning constants: λ_1, λ_2

Number of k-space samples added at each iteration: N_k

Expected fidelity of measurements: \mathbf{A}

Output: Estimated image: \hat{x}

Initialize:

$\mathbf{W}_1 = \mathbf{I}$, $\mathbf{W}_2 = \mathbf{I}$;

Reconstruction:

while $\mathbf{z} \neq \emptyset$ **do**

Move N_k new samples to \mathbf{y} from \mathbf{z} according to distance from center of k-space.

Weighted reconstruction: Estimate \hat{x} by solving (8)

Update weights: Update \mathbf{W}_1 and \mathbf{W}_2 according to (11)
end while

Algorithm 4 SFISTA algorithm for solving (8)

Input:

k-space measurements: \mathbf{y}

Sparsifying transform operator: Ψ_3

Fourier operator: \mathbf{F}_3

Expected fidelity of measurements: \mathbf{A}

Tuning constants: $\lambda_1, \lambda_2, \mu$

An upper bound: $L \geq \|\mathbf{A}\mathbf{F}_3\|_2^2 + \frac{\|\mathbf{W}_1 \Psi_3\|_2^2 + \|\mathbf{W}_2 \mathbf{B}\|_2^2}{\mu}$

Output: Estimated image: \hat{x}

Initialize:

$\mathbf{x}_1 = \mathbf{z}_2 = \mathbf{F}_3^* \mathbf{y}$, $t_2 = 1$

Iterations:

Step k: ($k \geq 2$) Compute

$$\nabla f(\mathbf{z}_k) = \mathbf{A}^* (\mathbf{F}_3^* (\mathbf{A} (\mathbf{F}_3 \mathbf{z}_k - \mathbf{y})))$$

$$\nabla g_{1\mu}(\mathbf{W}_1 \Psi_3 \mathbf{x}_{k-1}) = \frac{1}{\mu} \mathbf{W}_1 \Psi_3^* (\mathbf{W}_1 \Psi_3 \mathbf{x}_{k-1} - \Gamma_{\lambda_1 \mu} (\mathbf{W}_1 \Psi_3 \mathbf{x}_{k-1}))$$

$$\nabla g_{2\mu}(\mathbf{W}_2 \mathbf{B} \mathbf{x}_{k-1}) = \frac{1}{\mu} \mathbf{W}_2 \mathbf{B}^* (\mathbf{W}_2 \mathbf{B} \mathbf{x}_{k-1} - \Gamma_{\lambda_2 \mu} (\mathbf{W}_2 \mathbf{B} \mathbf{x}_{k-1}))$$

$$\mathbf{x}_k = \mathbf{z}_k - \frac{1}{L} (\nabla f(\mathbf{z}_k) + \nabla g_{1\mu}(\mathbf{W}_1 \Psi_3 \mathbf{x}_{k-1}) + \nabla g_{2\mu}(\mathbf{W}_2 \mathbf{B} \mathbf{x}_{k-1}))$$

$$t_{k+1} = \frac{1 + \sqrt{1 + 4t_k^2}}{2}$$

REFERENCES

- [1] Emmanuel J Candès, "Compressive sampling," in *Proceedings of the International Congress of Mathematicians: Madrid, August 22-30, 2006: invited lectures*, 2006, pp. 1433–1452.
- [2] D. L. Donoho, "Compressed sensing," *IEEE Transactions on Information Theory*, vol. 52, no. 4, pp. 1289–1306, 2006.
- [3] Yonina C Eldar and Gitta Kutyniok, *Compressed sensing: theory and applications*, Cambridge University Press, 2012.
- [4] Yonina C Eldar, *Sampling Theory: Beyond Bandlimited Systems*, Cambridge University Press, 2015.
- [5] Michael Lustig, David Donoho, and John M Pauly, "Sparse mri: The application of compressed sensing for rapid mr imaging," *Magnetic resonance in medicine*, vol. 58, no. 6, pp. 1182–1195, 2007.
- [6] Shiqian Ma, Wotao Yin, Yin Zhang, and Amit Chakraborty, "An efficient algorithm for compressed mr imaging using total variation and wavelets," in *Computer Vision and Pattern Recognition, 2008. CVPR 2008. IEEE Conference on*, IEEE, 2008, pp. 1–8.
- [7] Urs Gamper, Peter Boesiger, and Sebastian Kozerke, "Compressed sensing in dynamic mri," *Magnetic Resonance in Medicine*, vol. 59, no. 2, pp. 365–373, 2008.
- [8] Ricardo Otazo, Emmanuel Candès, and Daniel K Sodickson, "Low-rank plus sparse matrix decomposition for accelerated dynamic MRI with separation of background and dynamic components," *Magnetic Resonance in Medicine*, vol. 73, no. 3, pp. 1125–1136, 2015.
- [9] Mark Chiew, Stephen M Smith, Peter J Koopmans, Nadine N Graedel, Thomas Blumensath, and Karla L Miller, "k-t faster: Acceleration of functional MRI data acquisition using low rank constraints," *Magnetic Resonance in Medicine*, 2014.
- [10] Berkin Bilgic, Vivek K Goyal, and Elfar Adalsteinsson, "Multi-contrast reconstruction with bayesian compressed sensing," *Magnetic Resonance in Medicine*, vol. 66, no. 6, pp. 1601–1615, 2011.
- [11] Junzhou Huang, Chen Chen, and Leon Axel, "Fast multi-contrast MRI reconstruction," *Magnetic resonance imaging*, vol. 32, no. 10, pp. 1344–1352, 2014.
- [12] Lior Weizman, Yonina C Eldar, and Dafna Ben Bashat, "Compressed sensing for longitudinal MRI: An adaptive weighted approach," *Medical Physics*, vol. 42, no. 9, 2015, to appear, available at <http://arxiv.org/abs/1407.2602>.
- [13] S. Ravishankar and Y. Bresler, "Adaptive sampling design for compressed sensing MRI," in *2011 Annual International Conference of the IEEE Engineering in Medicine and Biology Society*. IEEE, 2011, pp. 3751–3755.
- [14] Lior Weizman, Ohad Rahamim, Roey Dekel, Yonina C Eldar, and Dafna Ben-Bashat, "Exploiting similarity in adjacent slices for compressed sensing MRI," in *36th Annual International Conference of the IEEE Engineering in Medicine and Biology Society (EMBC), 2014*. IEEE, 2014, pp. 1549–1552.
- [15] Tao Lang and Jim Ji, "Accelerating dynamic contrast-enhanced MRI using compressed sensing," in *Proceedings of the 16th annual meeting of ISMRM, Toronto, Canada*, 2008, p. 1481.
- [16] Hong Jung, Kyunghyun Sung, Krishna S Nayak, Eung Yeop Kim, and Jong Chul Ye, "k-t focuss: A general compressed sensing framework for high resolution dynamic MRI," *Magnetic Resonance in Medicine*, vol. 61, no. 1, pp. 103–116, 2009.
- [17] Michael Lustig, Juan M Santos, David L Donoho, and John M Pauly, "K-T sparse: High frame rate dynamic MRI exploiting spatio-temporal sparsity," in *Proceedings of the 13th Annual Meeting of ISMRM, Seattle, 2006*, vol. 2420.
- [18] Emmanuel J Candès, Michael B Wakin, and Stephen P Boyd, "Enhancing sparsity by reweighted l1 minimization," *Journal of Fourier analysis and applications*, vol. 14, no. 5-6, pp. 877–905, 2008.
- [19] Zhao Tan, Yonina C Eldar, Amir Beck, and Arye Nehorai, "Smoothing and decomposition for analysis sparse recovery," *IEEE Transactions on Signal Processing*, vol. 62, no. 7, pp. 1762–1774, 2014.
- [20] Gary P Zientara, Lawrence P Panych, and Ferenc A Jolesz, "Dynamically adaptive mri with encoding by singular value decomposition," *Magnetic Resonance in Medicine*, vol. 32, no. 2, pp. 268–274, 1994.
- [21] Scott K Nagle and David N Levin, "Multiple region mri," *Magnetic resonance in medicine*, vol. 41, no. 4, pp. 774–786, 1999.
- [22] Yun Gao and Stanley J Reeves, "Optimal k-space sampling in mri for images with a limited region of support," *Medical Imaging, IEEE Transactions on*, vol. 19, no. 12, pp. 1168–1178, 2000.
- [23] Jarvis Haupt, Robert Nowak, and Rui Castro, "Adaptive sensing for sparse signal recovery," in *IEEE 13th Digital Signal Processing Workshop and 5th IEEE Signal Processing Education Workshop, 2009. DSP/SPE 2009*. IEEE, 2009, pp. 702–707.

- [24] Jarvis Haupt, Rui M Castro, and Robert Nowak, "Distilled sensing: Adaptive sampling for sparse detection and estimation," *IEEE Transactions on Information Theory*, vol. 57, no. 9, pp. 6222–6235, 2011.
- [25] Dennis Wei and Alfred O Hero, "Multistage adaptive estimation of sparse signals," *IEEE Journal of Selected Topics in Signal Processing*, vol. 7, no. 5, pp. 783–796, 2013.
- [26] Matthias Seeger, Hannes Nickisch, Rolf Pohmann, and Bernhard Schölkopf, "Optimization of k-space trajectories for compressed sensing by bayesian experimental design," *Magnetic resonance in medicine*, vol. 63, no. 1, pp. 116–126, 2010.
- [27] Yue Cao and David N Levin, "Feature-recognizing MRI," *Magnetic resonance in medicine*, vol. 30, no. 3, pp. 305–317, 1993.
- [28] Alon Eilan, "personal communication," April 2015.